

Damage assessment and vulnerability modeling of structures in the 2016 Kumamoto earthquake based on the data acquired from field investigation and remote sensing

現地調査とリモートセンシングを融合した熊本地震による構造物の被害把握と被害予測モデル構築

March 4, 2017



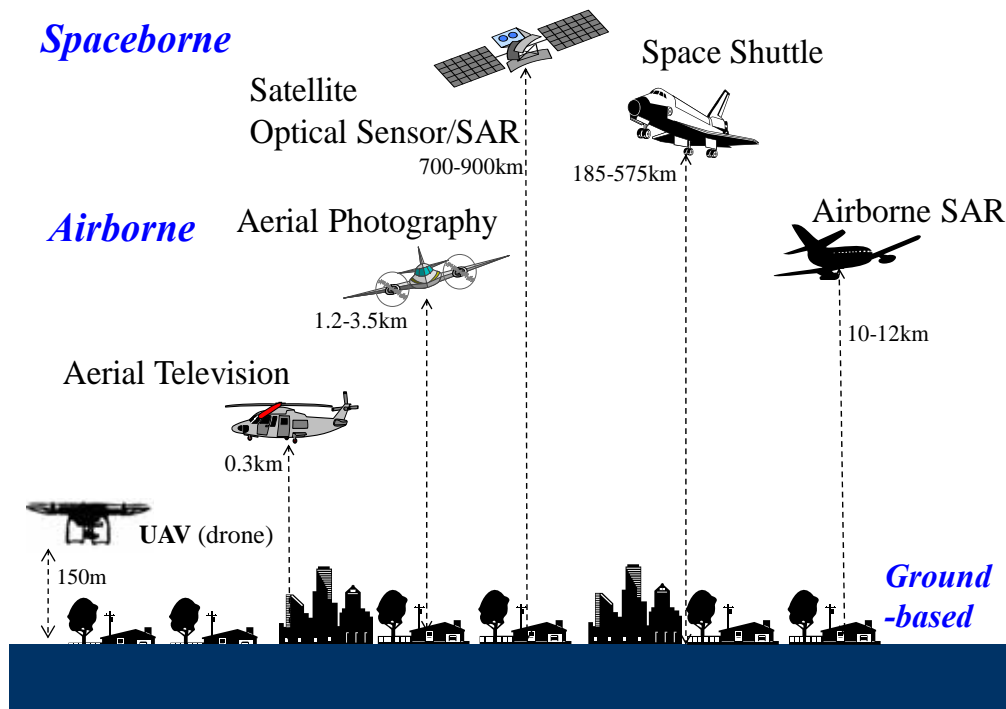
Fumio Yamazaki

Professor, Chiba University, Japan

1

Platforms of Remote Sensing

- **Satellite:** near-polar orbit, geo-stationary, Space Shuttle
- **Airborne platform:** airplane, helicopter, UAV
- **Ground-based:** balloon, tall building, crane, ladder, car



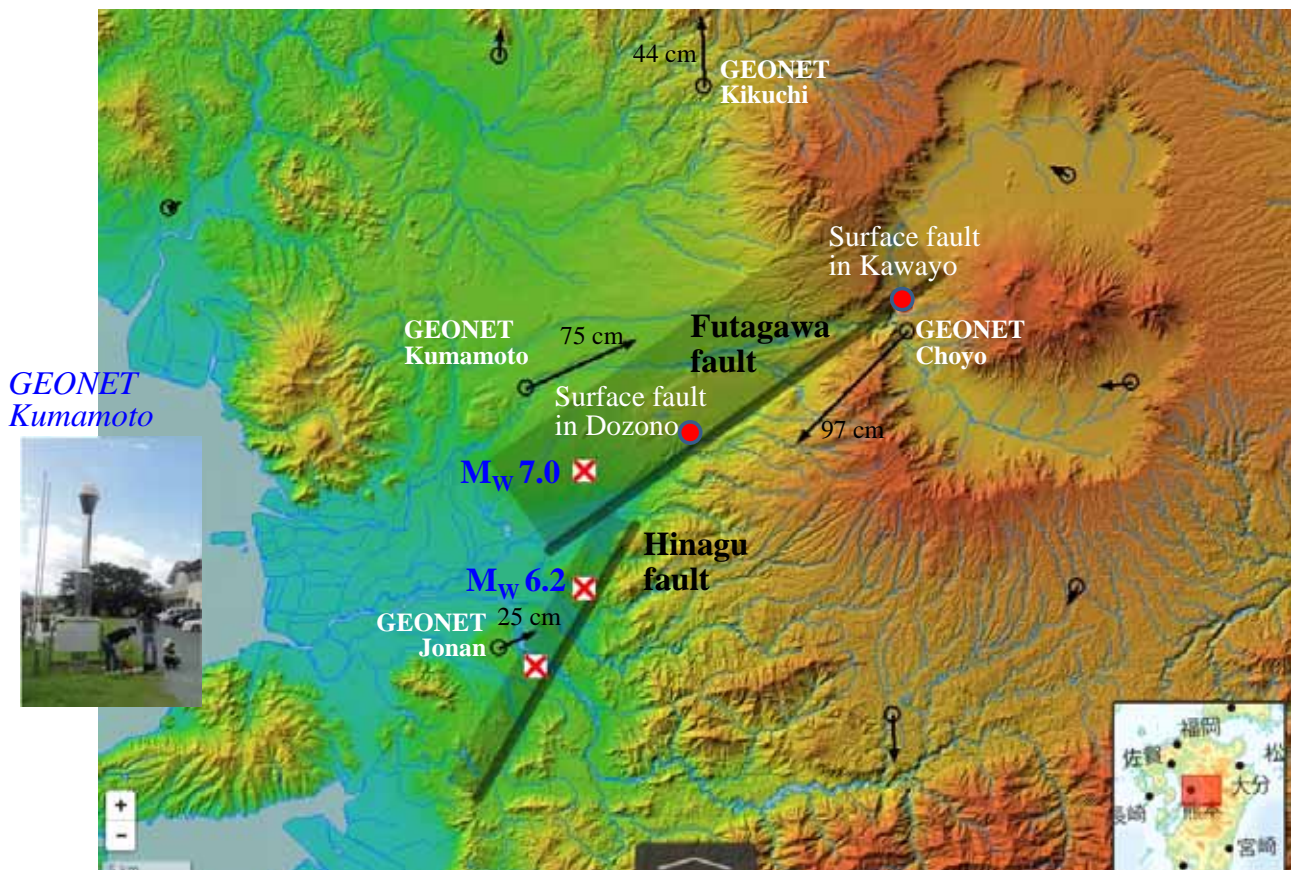
2

Acquisition condition of various sensors and platforms in disaster response

Platform /Sensor	Satellite Large coverage	Airborne Mod. coverage	Ground Based Low coverage
Optical Sensor	Day, Fixed time No cloud	Day, Any time No low cloud	Day, Any time
LiDAR		All day, Any time No low cloud High accuracy	Day, Any time
Thermal Infrared	All day, Fixed time No cloud Low resolution	All day, Any time No low cloud Mod. resolution	All day, Any time High resolution
SAR	All day, Fixed time All weather	All day, Any time All weather R & D stage	Ground penetration Radar

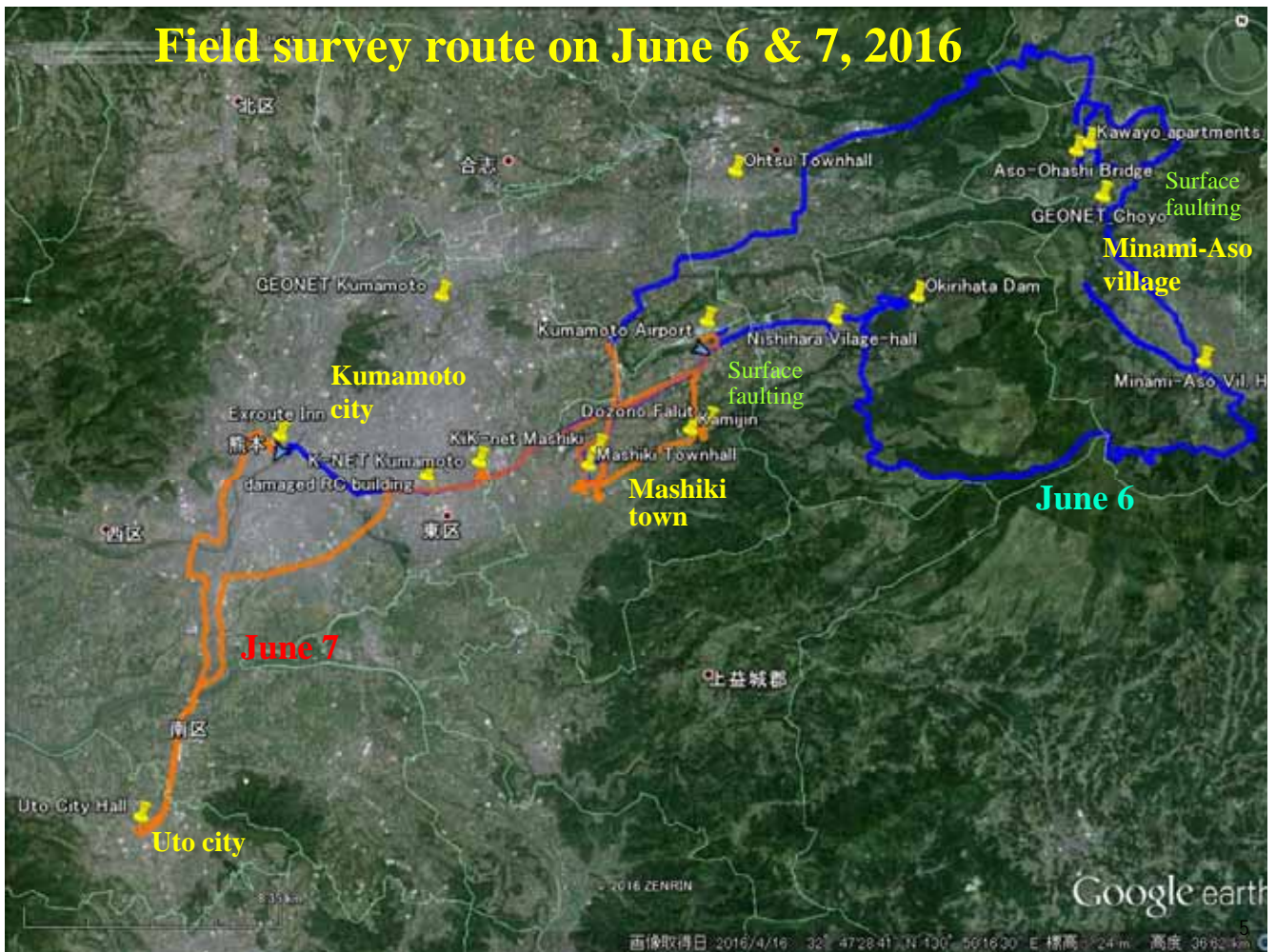
3

Epicenters, faults, and GPS stations in the 2016 Kumamoto EQ



4

Field survey route on June 6 & 7, 2016



Surface faulting in Mashiki town April 17



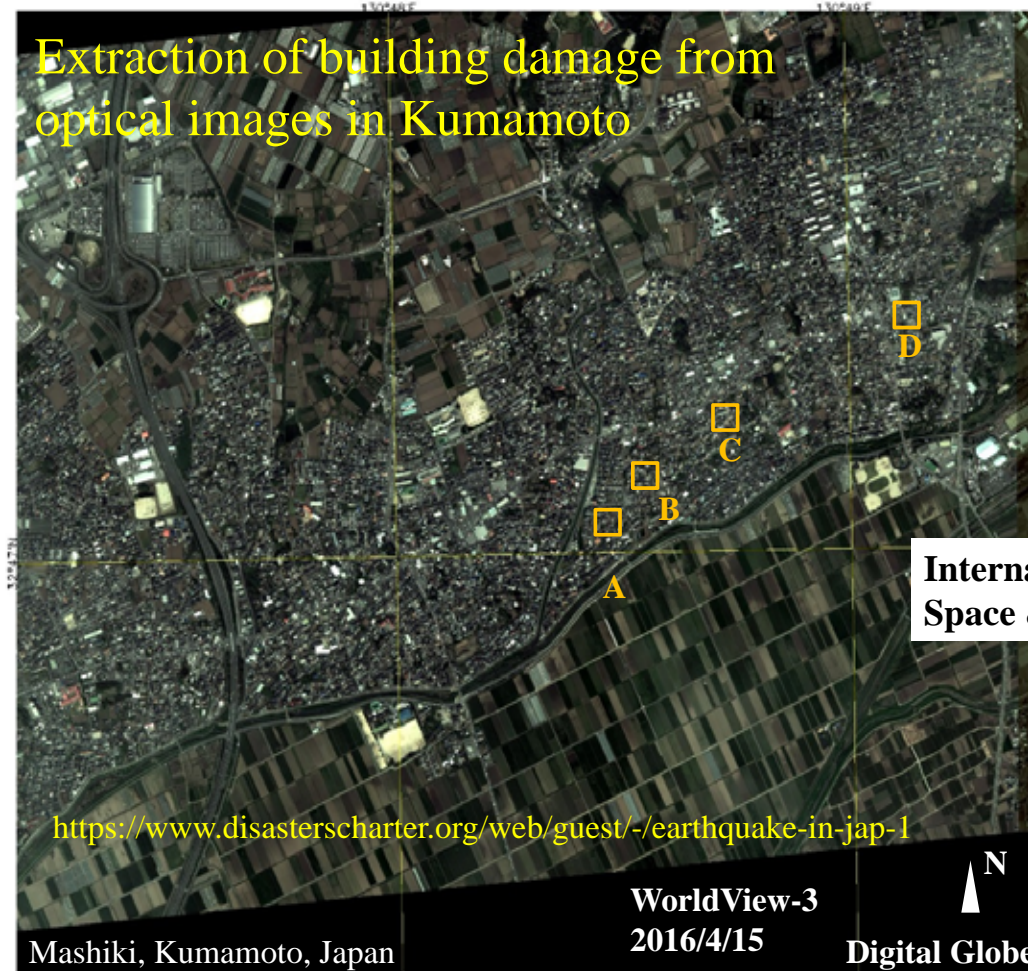
Building damage in Mashiki Town

April 16



7

Extraction of building damage from optical images in Kumamoto



International Charter –
Space & Major Disasters

<https://www.disasterscharter.org/web/guest/-/earthquake-in-jap-1>

WorldView-3
2016/4/15

Digital Globe



8

area A



2013/05/26



2016/4/15

Building Damage in Mashiki Town on April 15, 2016

Damaged buildings

Damaged buildings by visual interpretation from the pan-sharpened pre- and post-event optical images.

Pre-event: **WorldView-2**
2013/05/26
11:42:00 (JST)

Post-event: **WorldView-3**
2016/4/15
11:08:13 (JST)

Resolution: 0.5-m

WV2 and WV3 images are owned by Digital Globe and provided by USGS.

area B

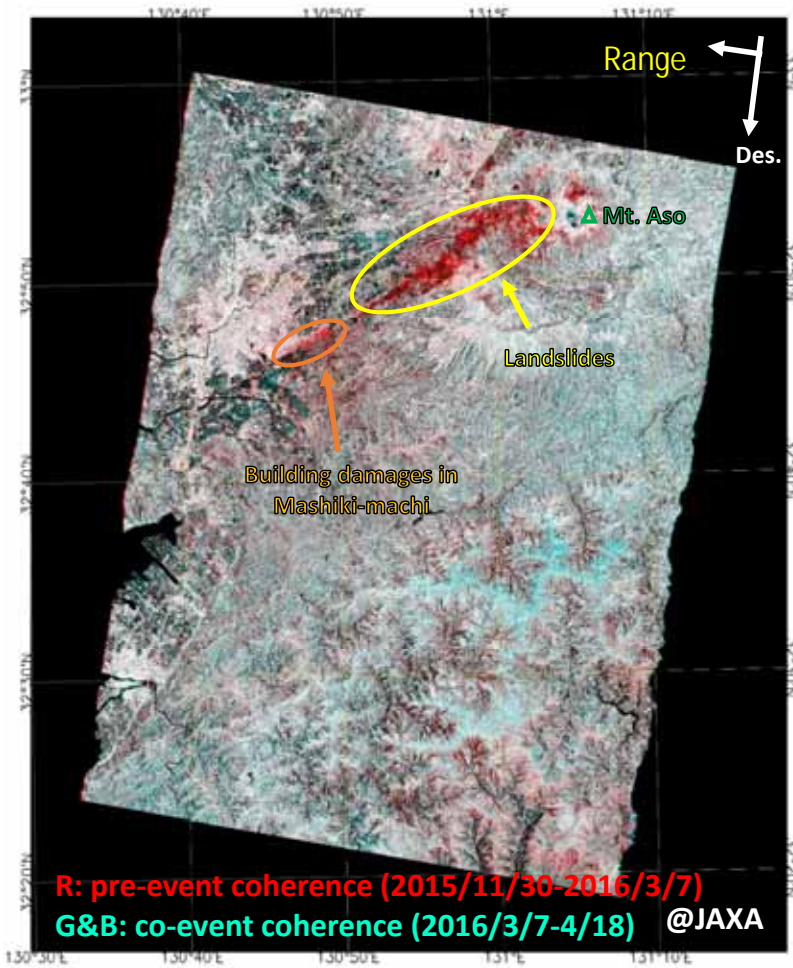


Monitoring of evacuation sites by VHR optical satellite images

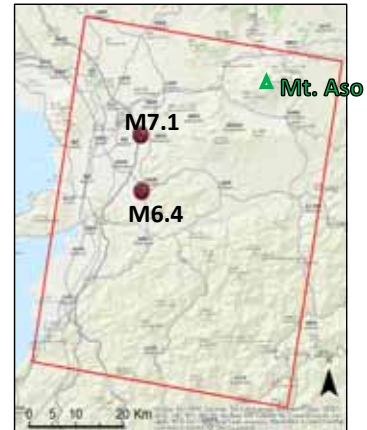
a. Hiroyasu-Nishi Primary School

益城町 広安西小学校

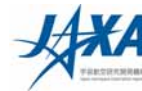




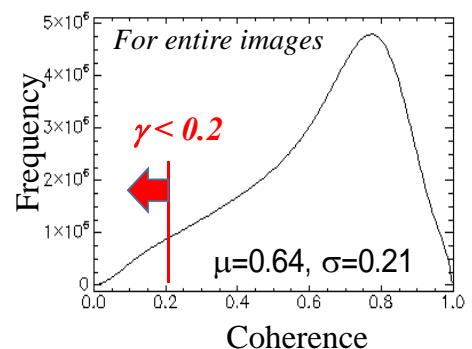
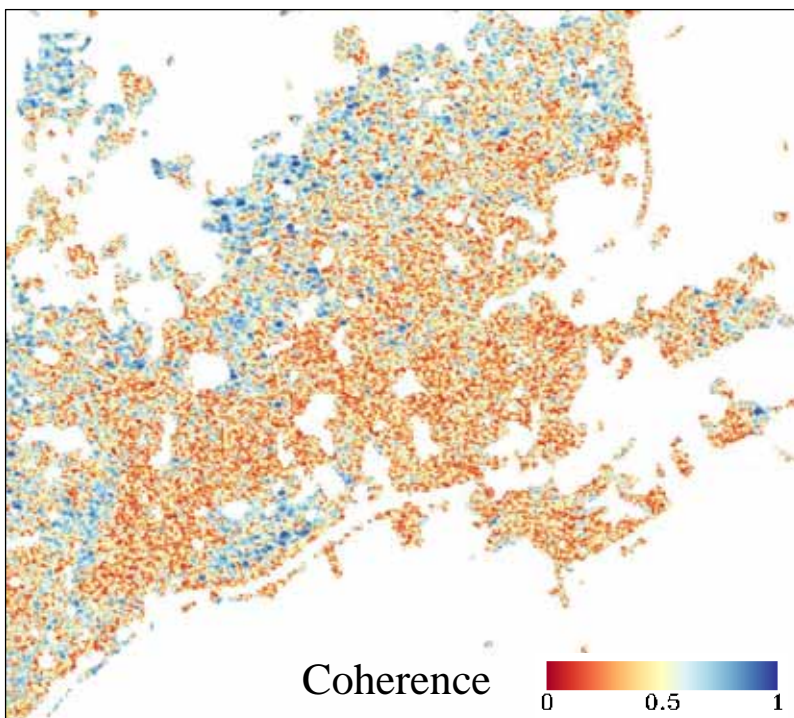
Color composite of the pre- and co-event PALSAR-2 coherence



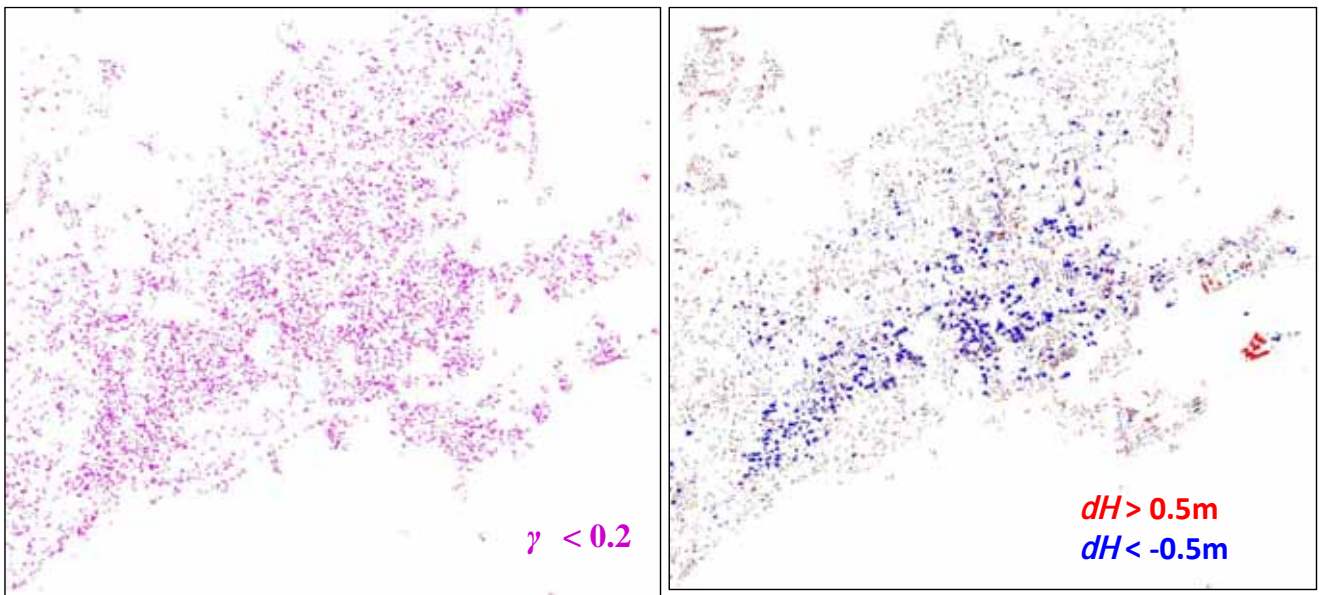
Pre-event: 2015/11/30, 2016/03/07
 Post-event: 2016/04/18
 Off-nadir angle: 32.4 °
 Mode: StripMap
 Polarization: HH



Coherence between the two PALSAR-2 images (2016/4/15 vs 2016/4/29) for the urban land-cover in the central Mashiki Town



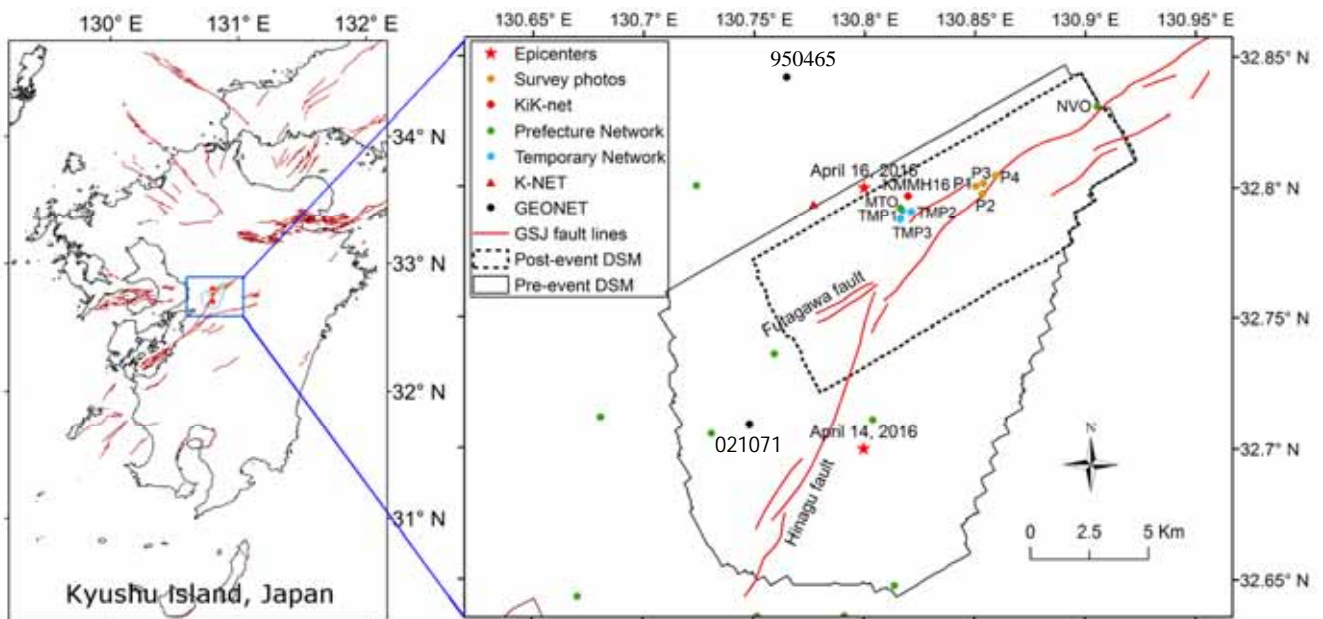
Changed areas extracted by low coherence ($\gamma < 0.2$) (a); and extracted by DSM height-difference (abs. (dH) > 0.5 m) (b)



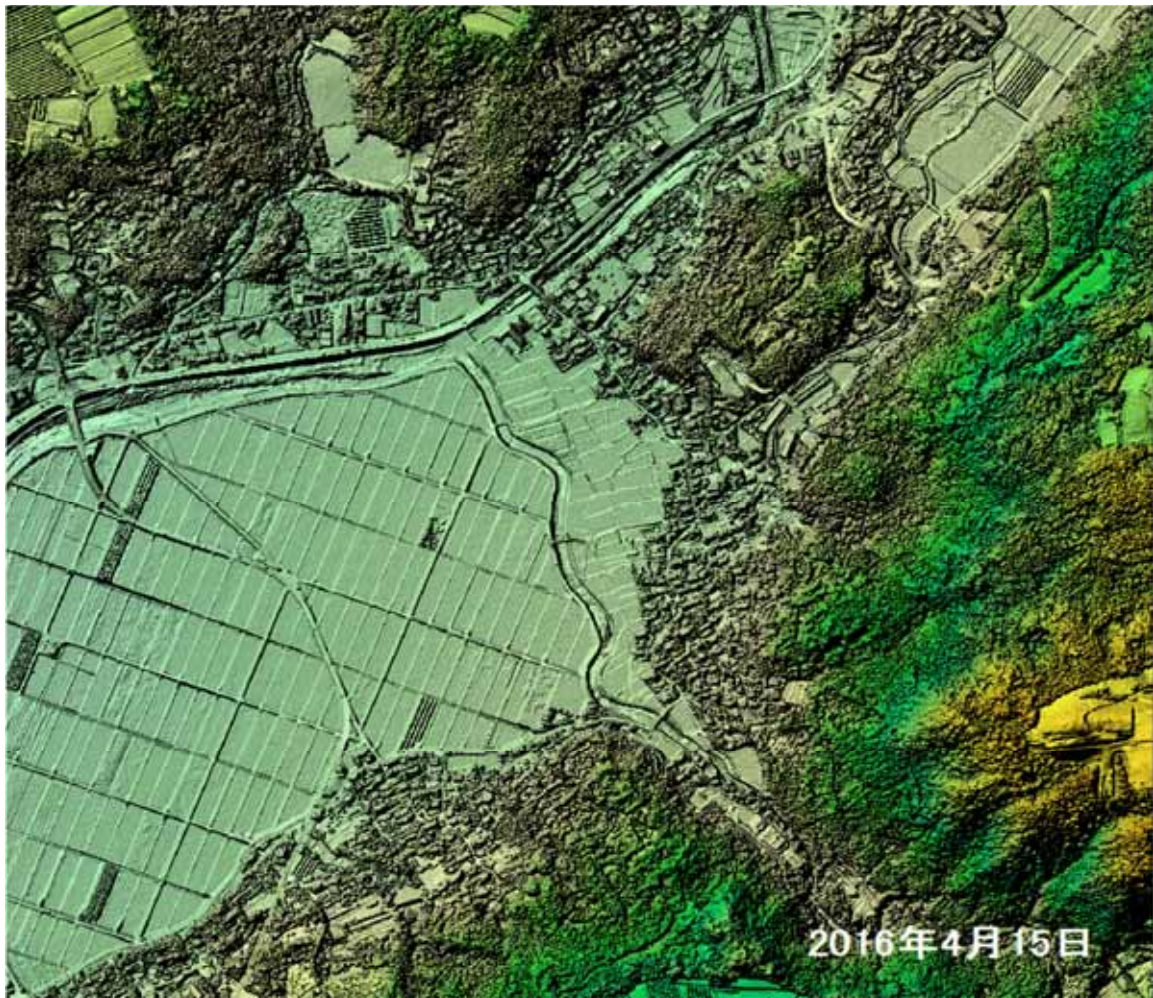
(a) Low coherence from SAR pair ($\gamma < 0.2$)

(b) LiDAR DSM height-difference (abs. (dH) > 0.5 m)

LiDAR SURVEYING FLIGHTS BY ASIA AIR SURVEY CO.



- Pre-event DSM: April 15 (1 day after the foreshock, 2 points/m²).
- Post-event DSM: April 23 (7 days after the mainshock, 4 points/m²).
- Six strong-motion are located within the study area.

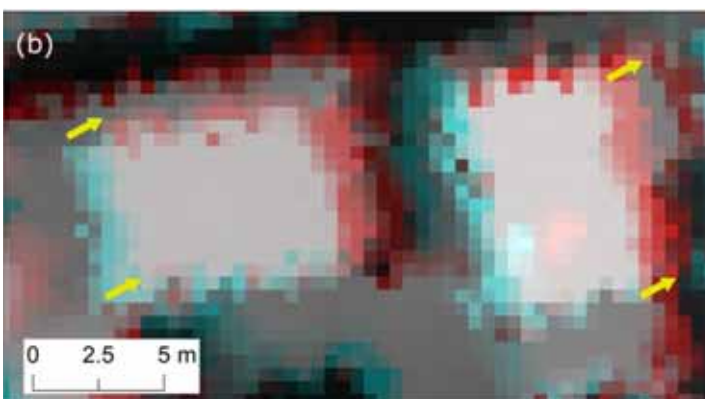


15

Color composite of the pre- and post-event LiDAR DSMs



Aerial image of buildings in Mashiki town



Crustal movement is observed as the shift of the DSM

Cyan pixels:

Pre-event DSM > post-event DSM

Red pixels:

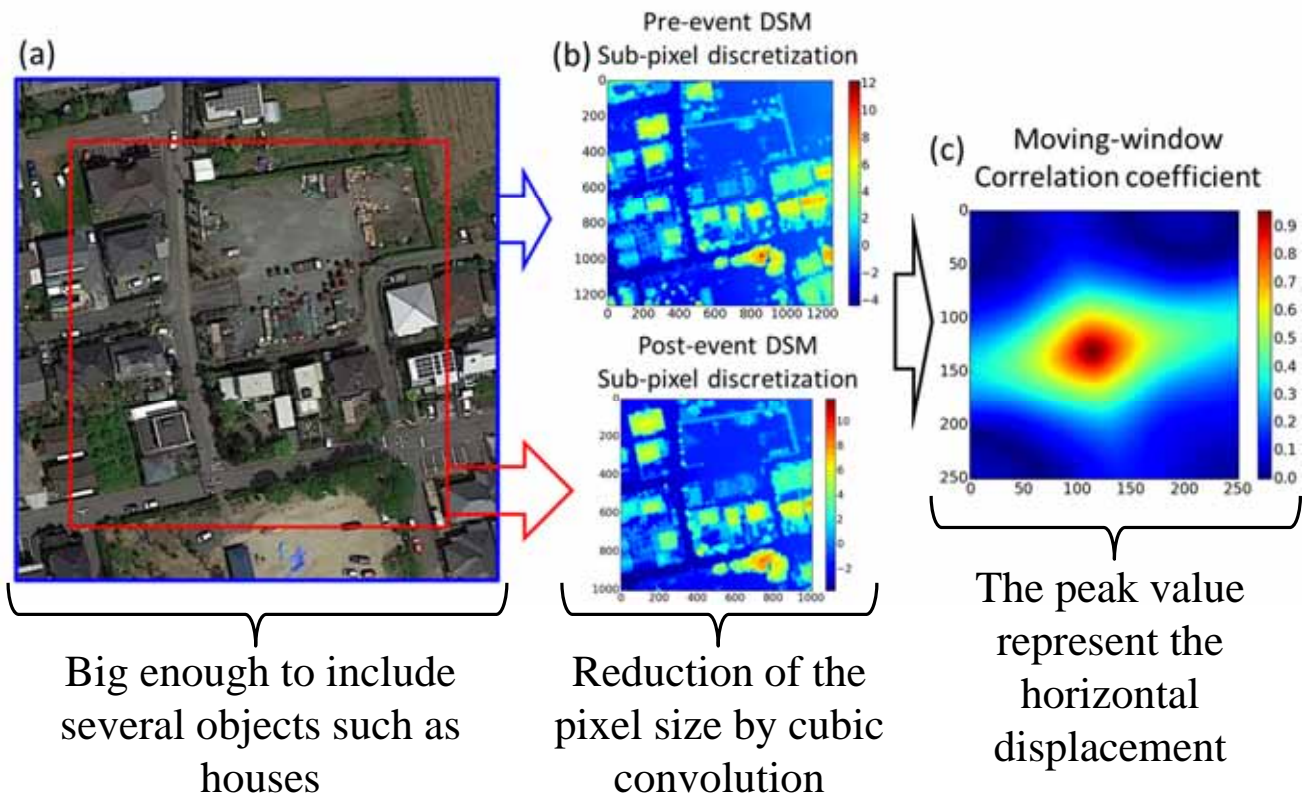
Pre-event DSM < post-event DSM

Gray pixels:

Pre-event DSM = post-event DSM

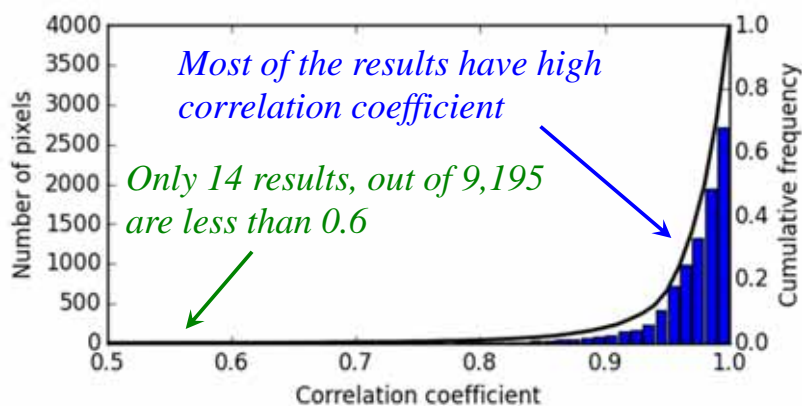
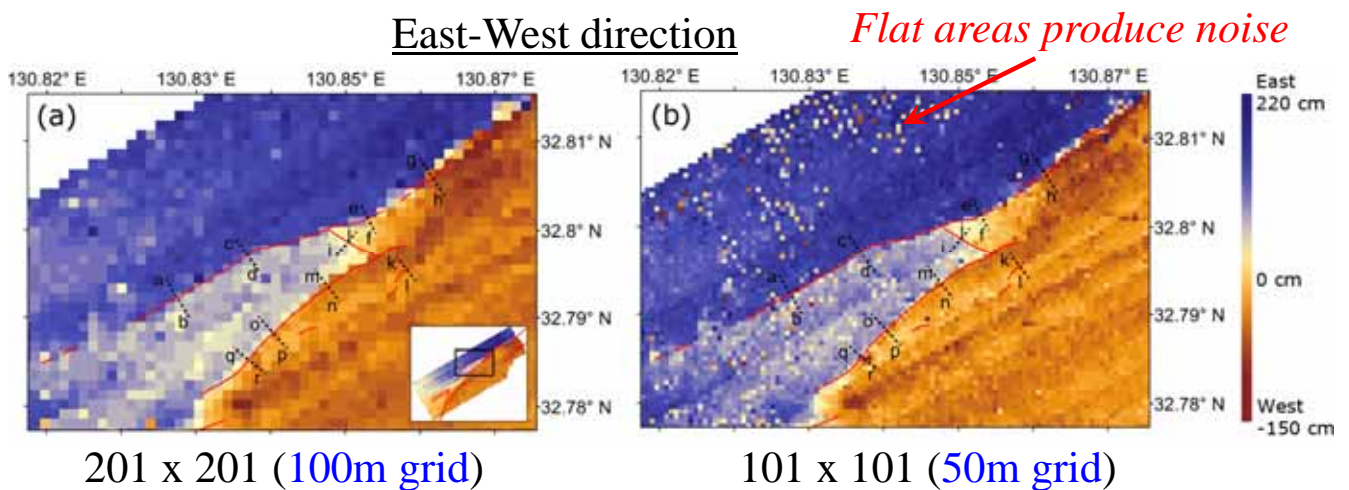
16

Scheme of the Maximum Correlation Search



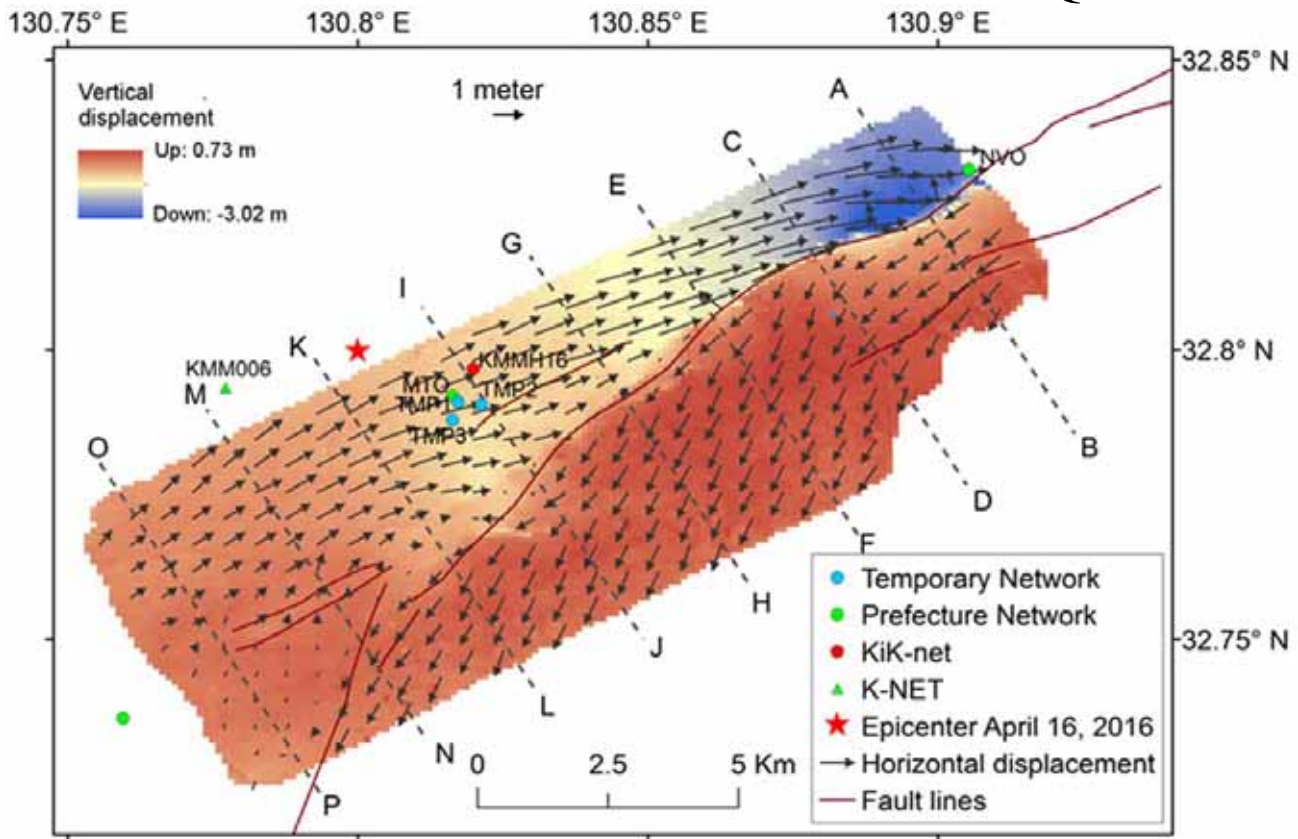
17

Window Size for Correlation Calculation



18

Estimated 3D coseismic displacement from LiDAR DSMs in the main-shock of the Kumamoto EQ

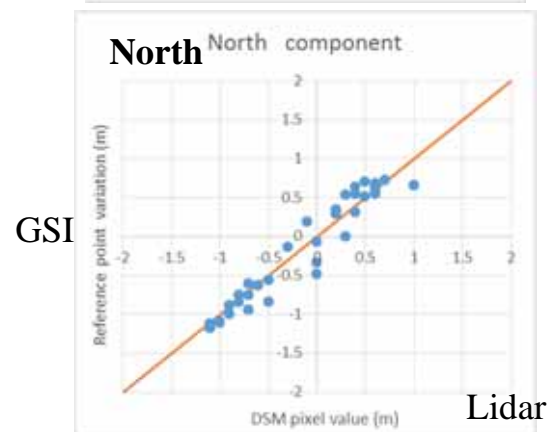
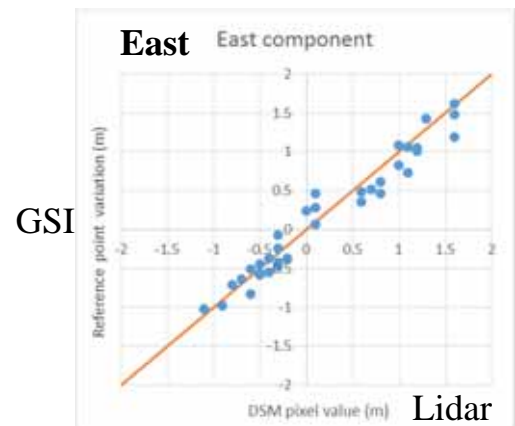


19

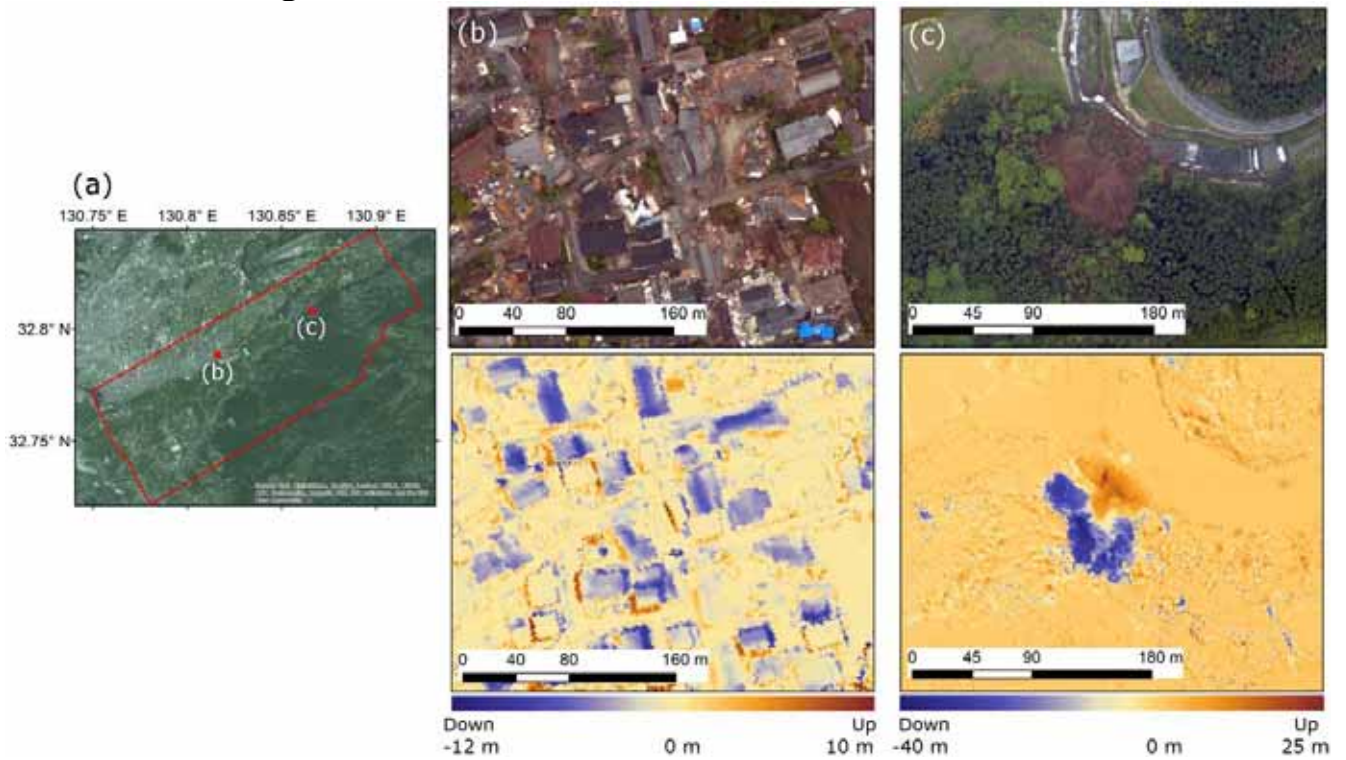
Comparison of LiDAR displacements with GSI's measurement



GSI's measurement
on August 30, 2016

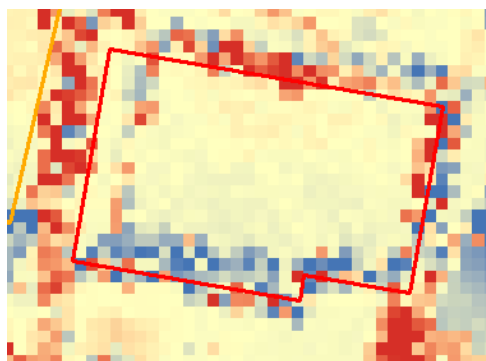


Extraction of collapsed buildings and landslide by the difference of LiDAR Digital Surface Models (DSMs)

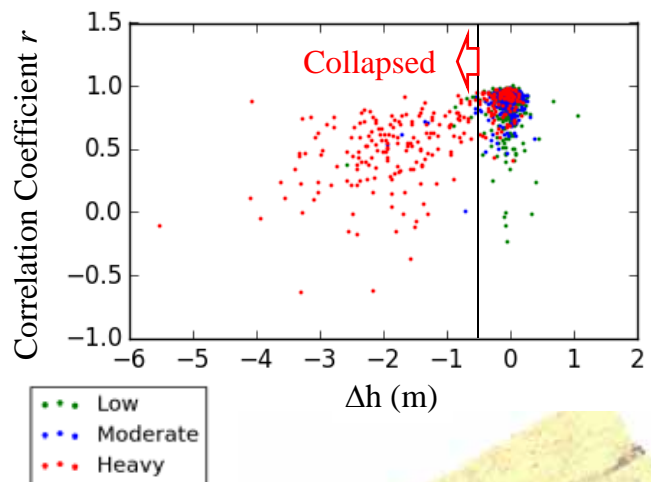


Moya, L., F. Yamazaki, W. Liu, T. Chiba, Estimation of coseismic displacement in the 2016 Kumamoto earthquake from Lidar data, *6ACEE*, 2016.

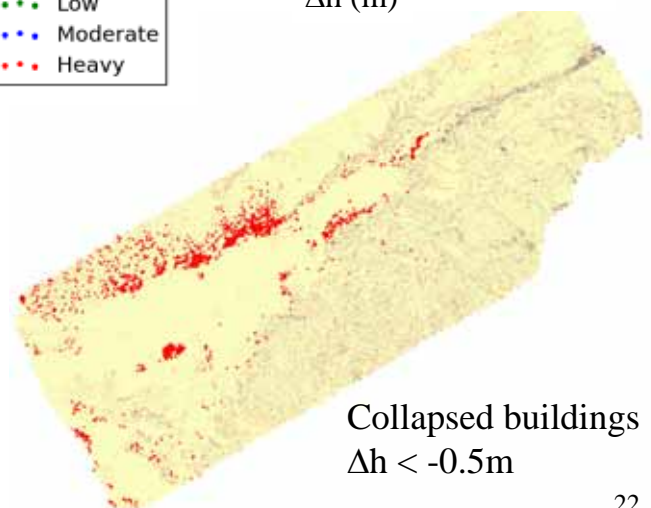
Estimation of collapsed buildings from the height change in the footprint



$\Delta h = -0.17\text{m}$ $\sigma = 0.77\text{m}$ $r = 0.857$



- Low
- Moderate
- Heavy



Collapsed buildings
 $\Delta h < -0.5\text{m}$

Summary

- Application of remote sensing technologies to disaster response was discussed for the 2016 Kumamoto, Japan earthquake.
- Optical satellite images were used under the framework of International Charter..
- Satellite SAR sensors were used to extract landslides and building damage.
- LiDAR DSMs were used to estimate detailed coseismic displacements, building damage and landslides.

References:

L. Moya, F. Yamazaki, W. Liu, T. Chiba, Calculation of coseismic displacement from Lidar data in the 2016 Kumamoto, Japan, earthquake, *Natural Hazards and Earth System Sciences*, 17, 143-156, 2017.

W. Liu, F. Yamazaki, Extraction of collapsed buildings due to the 2016 Kumamoto earthquake based on multi-temporal PALSAR-2 data, *Journal of Disaster Research*, 12(2), 2017.

F. Yamazaki, W. Liu, Remote sensing technologies for post-earthquake damage assessment: A case study on the 2016 Kumamoto earthquake, Keynote Lecture, *6th Asia Conference on Earthquake Engineering*, Cebu City, Philippines, 2016.

Symposium on J-Rapid-Kumamoto

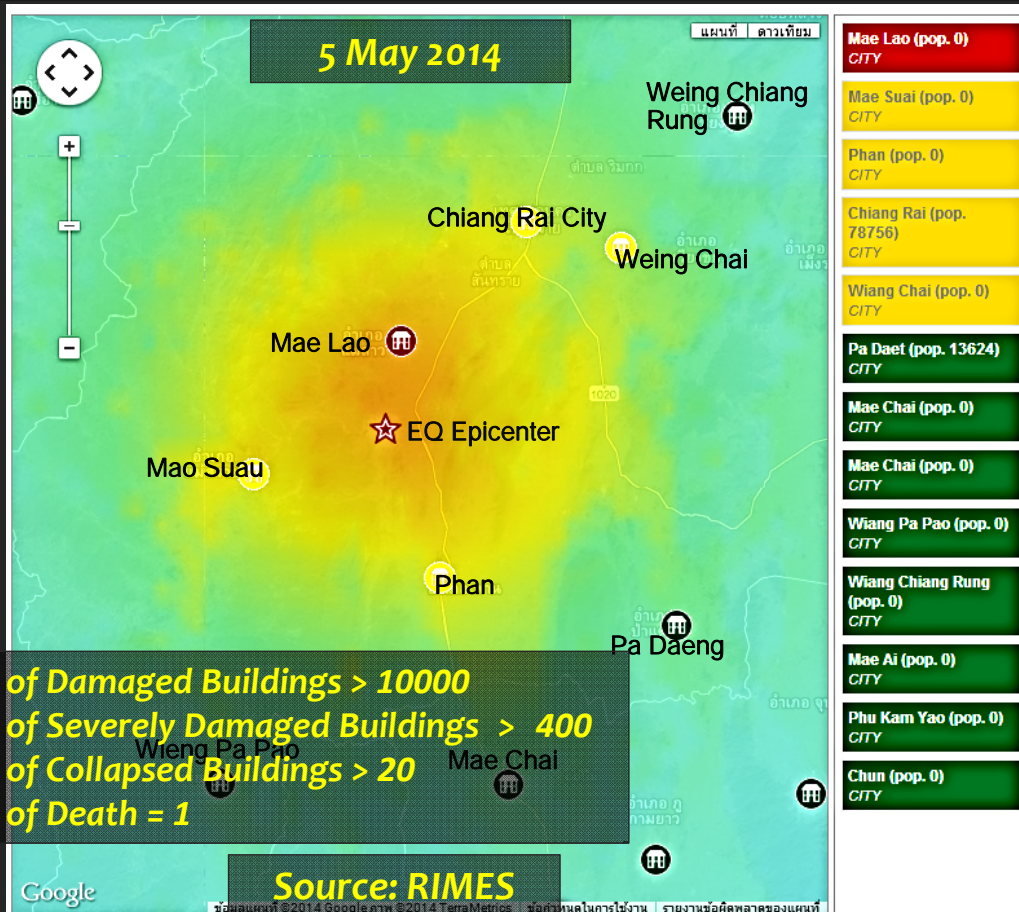
04 March 2017, Kumamoto University

Recent Earthquakes in Nepal, Thailand, and Japan *My impression about building vulnerability and ground motion*

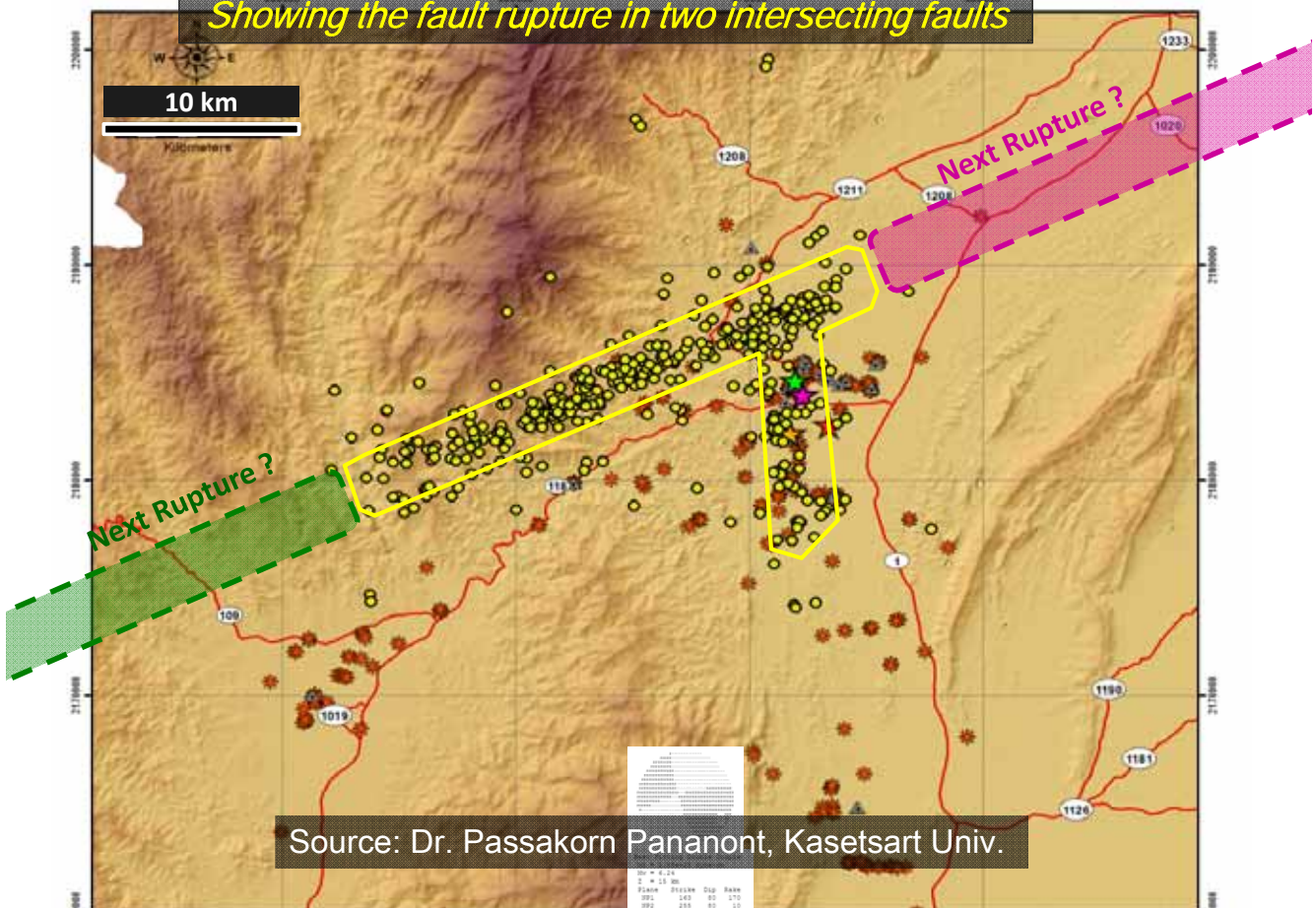
Pennung Warnitchai

*Professor of Structural Engineering
Asian Institute of Technology*

Ground Shaking Intensity Map of the M6.3 Chiang Rai Earthquake



Distribution of Aftershocks
Showing the fault rupture in two intersecting faults



Building collapse by the failure of all columns in the first story
(Ban Tamao, Mae Lao District, Chiang Rai: Epicentral Region)



**Phan Pithayakom School: a 4-story RC Building
(Phan District, Chiang Rai)**



Extensive shear failure in the first-story columns
No seismic detailing—low amount of transverse reinforcement & wide spacing
Failure location is just above the infill walls



Collapse of Masonry Infill Walls inside the Building

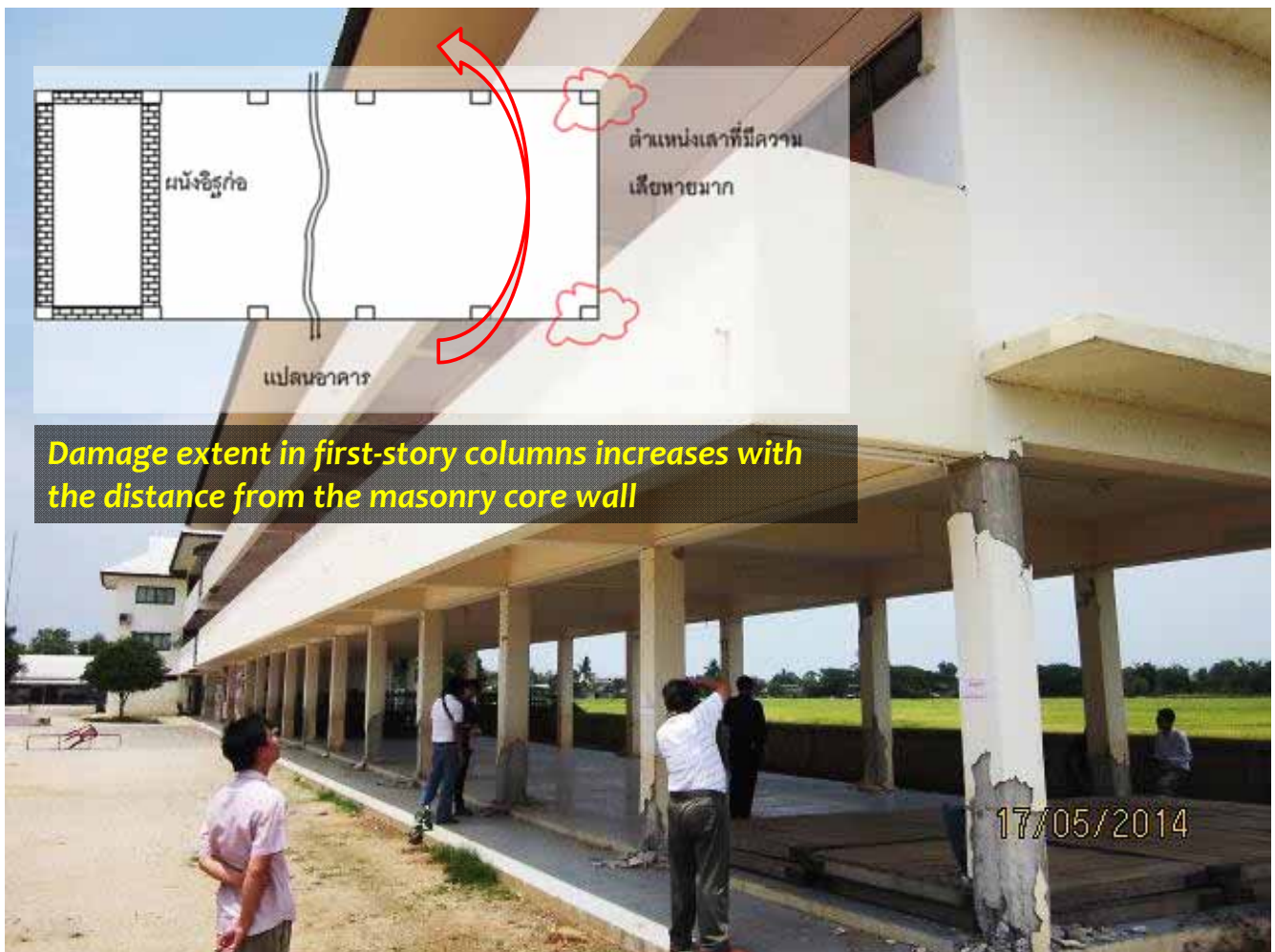


Collapse of Masonry Infill Walls inside the Building

Building occupants could be injured by the failure of non-structural components.



**Wat Muang Nga School: a 3-story RC Building
(Phan District, Chiang Rai)**



Failure Mode: Lap-splice Failure



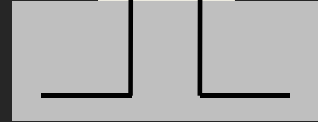
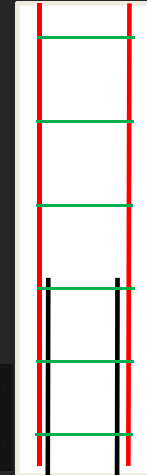
Column near core wall (no damage)



Column at center (moderately damage)



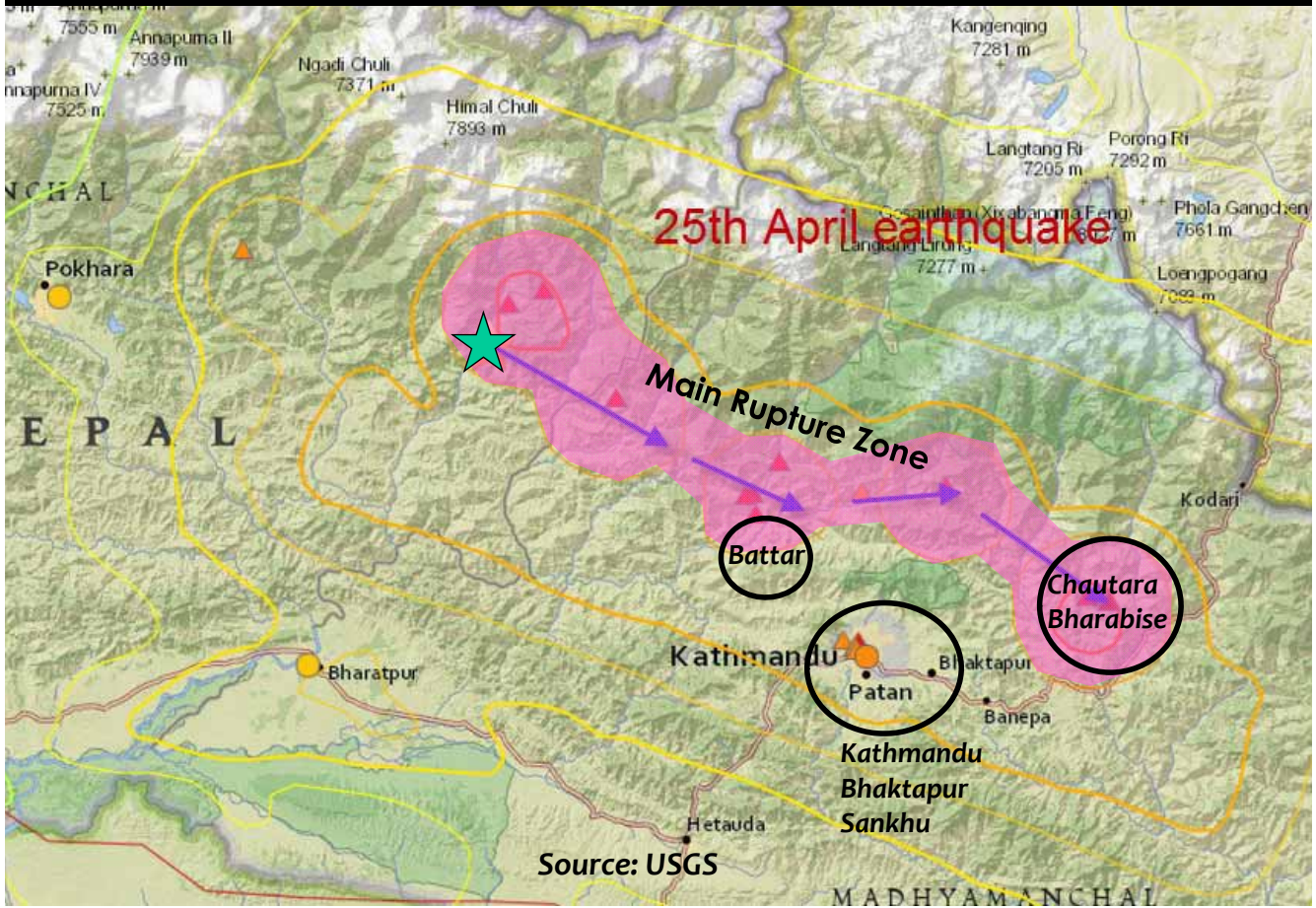
Column at right end (severely damage)



Nepal Earthquake: M 7.8, 25 April 2015



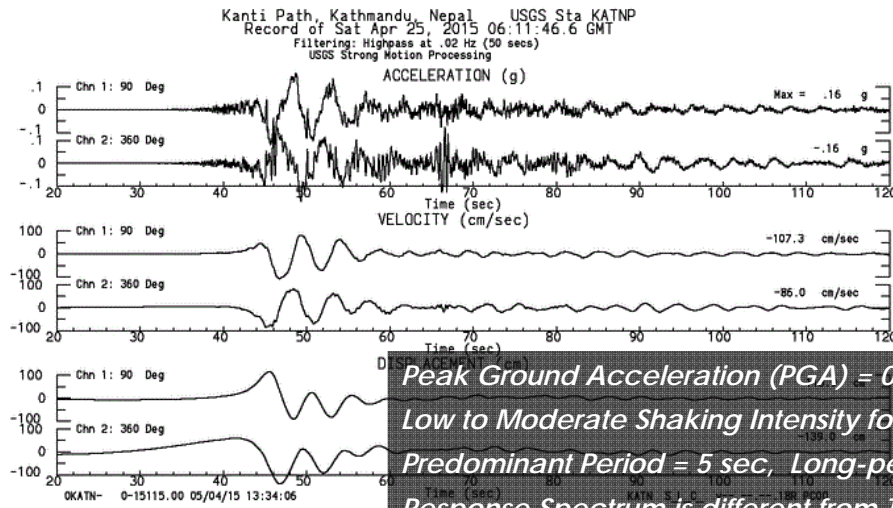
Rupture Mechanism



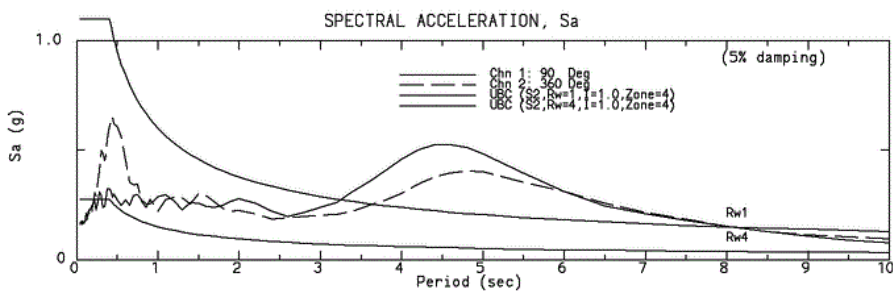
Kathmandu Valley View from Swayambhu Hill Top



Ground Motion Records in Kathmandu: The 25th April 2015 Earthquake (M_w 7.8)



Peak Ground Acceleration (PGA) = 0.16 g
Low to Moderate Shaking Intensity for Low-rise Buildings
Predominant Period = 5 sec, Long-period Ground Motion!
Response Spectrum is different from Typical Design Spectrum
More Damaging Effect to Tall Buildings (Long-period Structures)



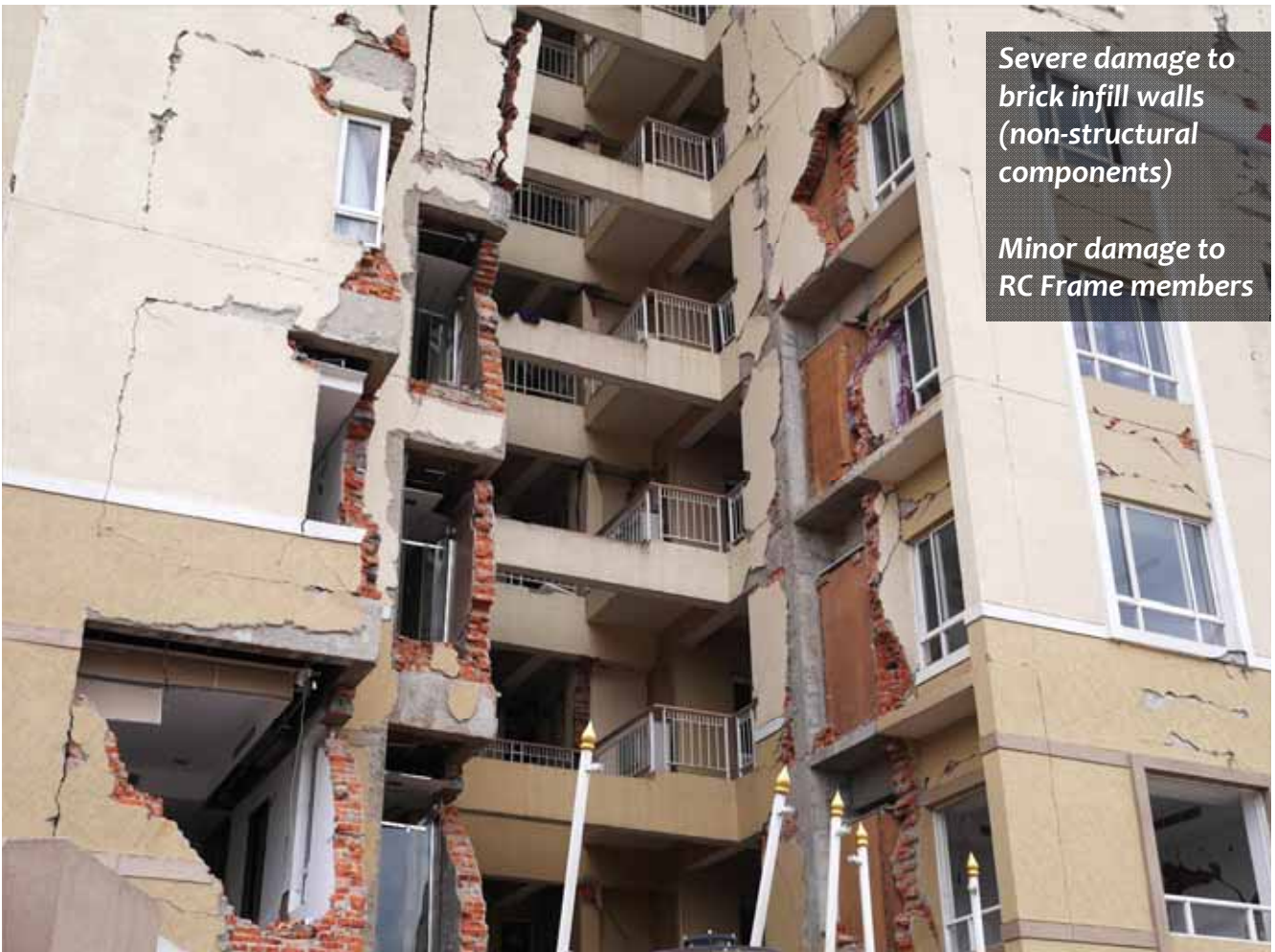
Minor or No Damage to Modern RC Buildings in Kathmandu City





**Park View Horizon Apartment
Kathmandu, Nepal**

**Damaged by the long-period
ground motion**



**Severe damage to
brick infill walls
(non-structural
components)**

**Minor damage to
RC Frame members**



All building occupants were evacuated from these buildings.

Should tall buildings be designed for long-period ground motions?

Should the seismic performance of non-structural components be considered in the seismic design of tall buildings?

Takai et al. *Earth, Planets and Space* (2016) 68:10
DOI 10.1186/s40623-016-0383-7

 Earth, Planets and Space
a SpringerOpen Journal

LETTER

Open Access

Strong ground motion in the Kathmandu Valley during the 2015 Gorkha, Nepal, earthquake

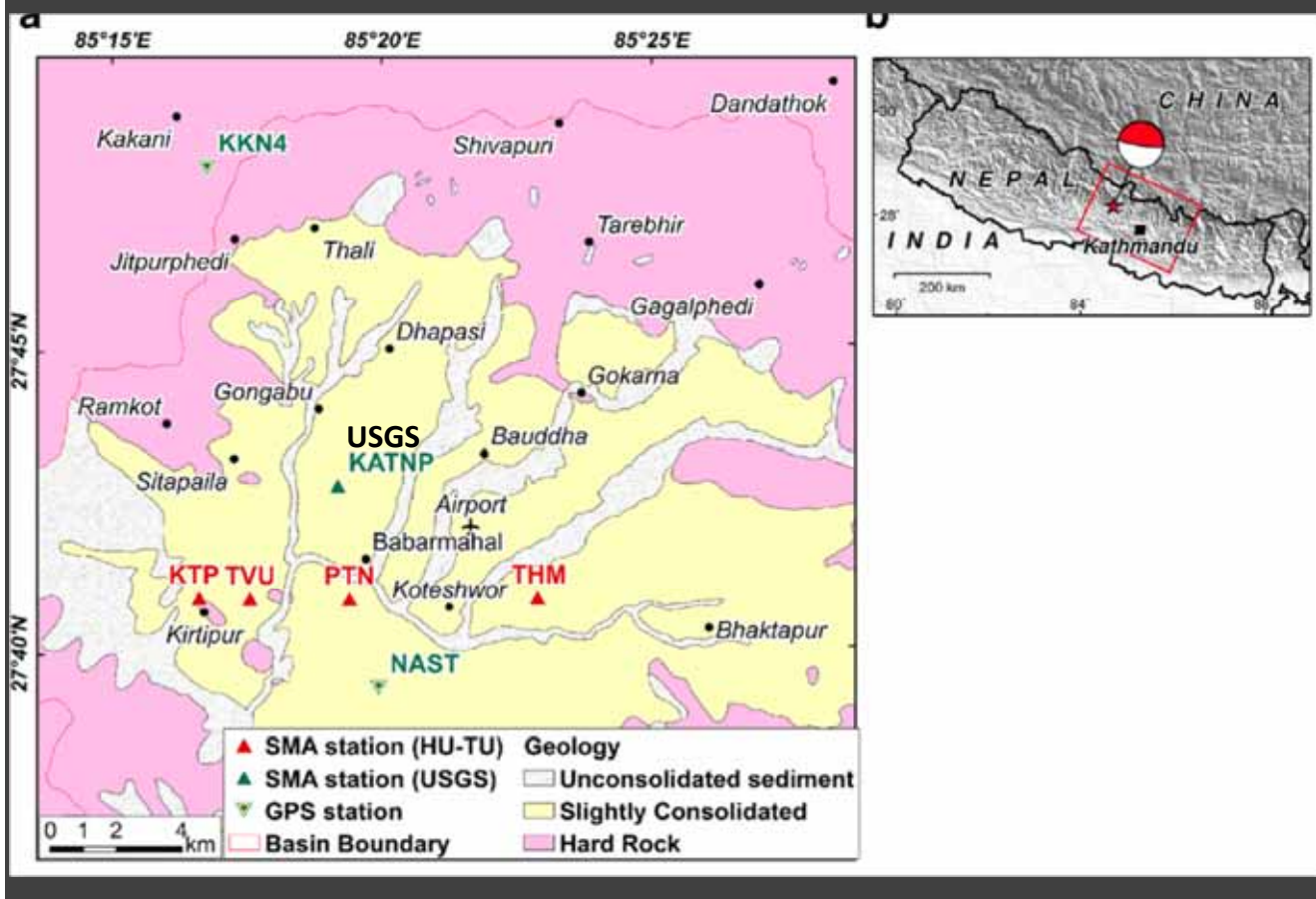


Nobuo Takai^{1*}, Michiko Shigefuji², Sudhir Rajaure³, Subeg Bijuochhen⁴, Masayoshi Ichiyanagi²,
Megh Raj Dhital⁵ and Tsutomu Sasatani⁶

Abstract

On 25 April 2015, a large earthquake of Mw 7.8 occurred along the Main Himalayan Thrust fault in central Nepal. It was caused by a collision of the Indian Plate beneath the Eurasian Plate. The epicenter was near the Gorkha region, 80 km northwest of Kathmandu, and the rupture propagated toward east from the epicentral region passing through the sediment-filled Kathmandu Valley. This event resulted in over 8000 fatalities, mostly in Kathmandu and the adjacent districts. We succeeded in observing strong ground motions at our four observation sites (one rock site and three sedimentary sites) in the Kathmandu Valley during this devastating earthquake. While the observed peak ground acceleration values were smaller than the predicted ones that were derived from the use of a ground motion prediction equation, the observed peak ground velocity values were slightly larger than the predicted ones. The ground velocities observed at the rock site (KTP) showed a simple velocity pulse, resulting in monotonic-step displacements associated with the permanent tectonic offset. The vertical ground velocities observed at the sedimentary sites had the same pulse motions that were observed at the rock site. In contrast the horizontal

Strong-motion Accelerometer Stations in Kathmandu Valley



Observed Ground Accelerations in Kathmandu

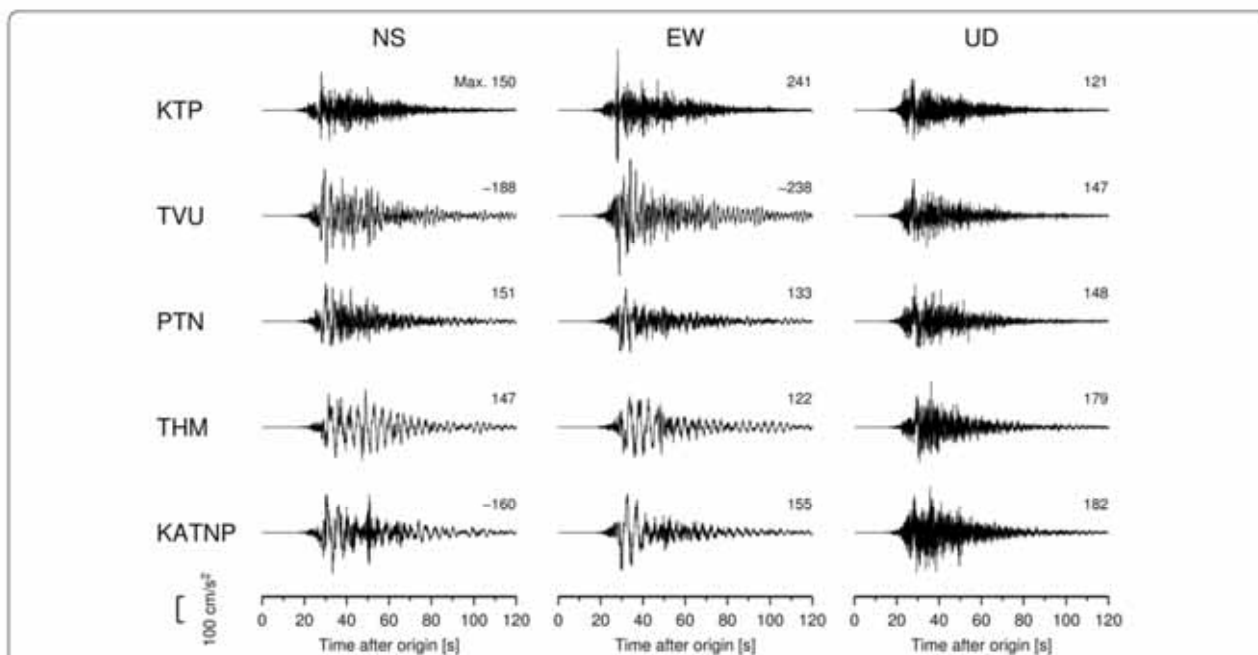
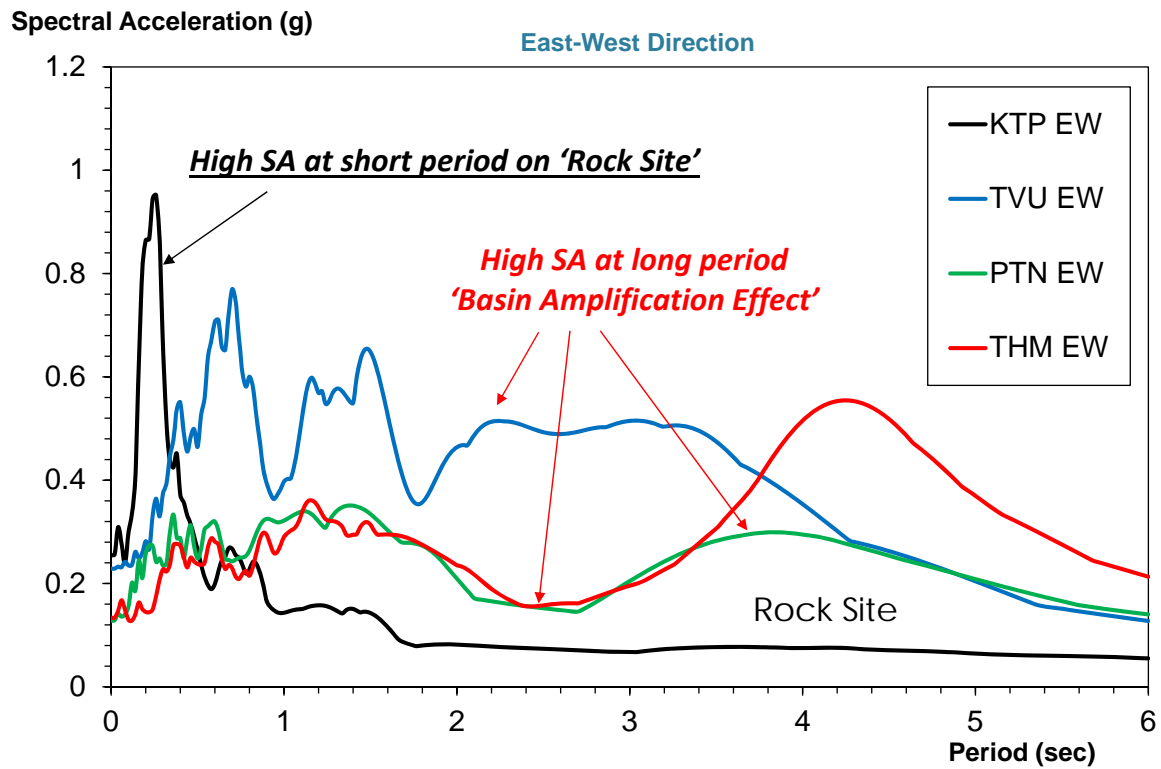


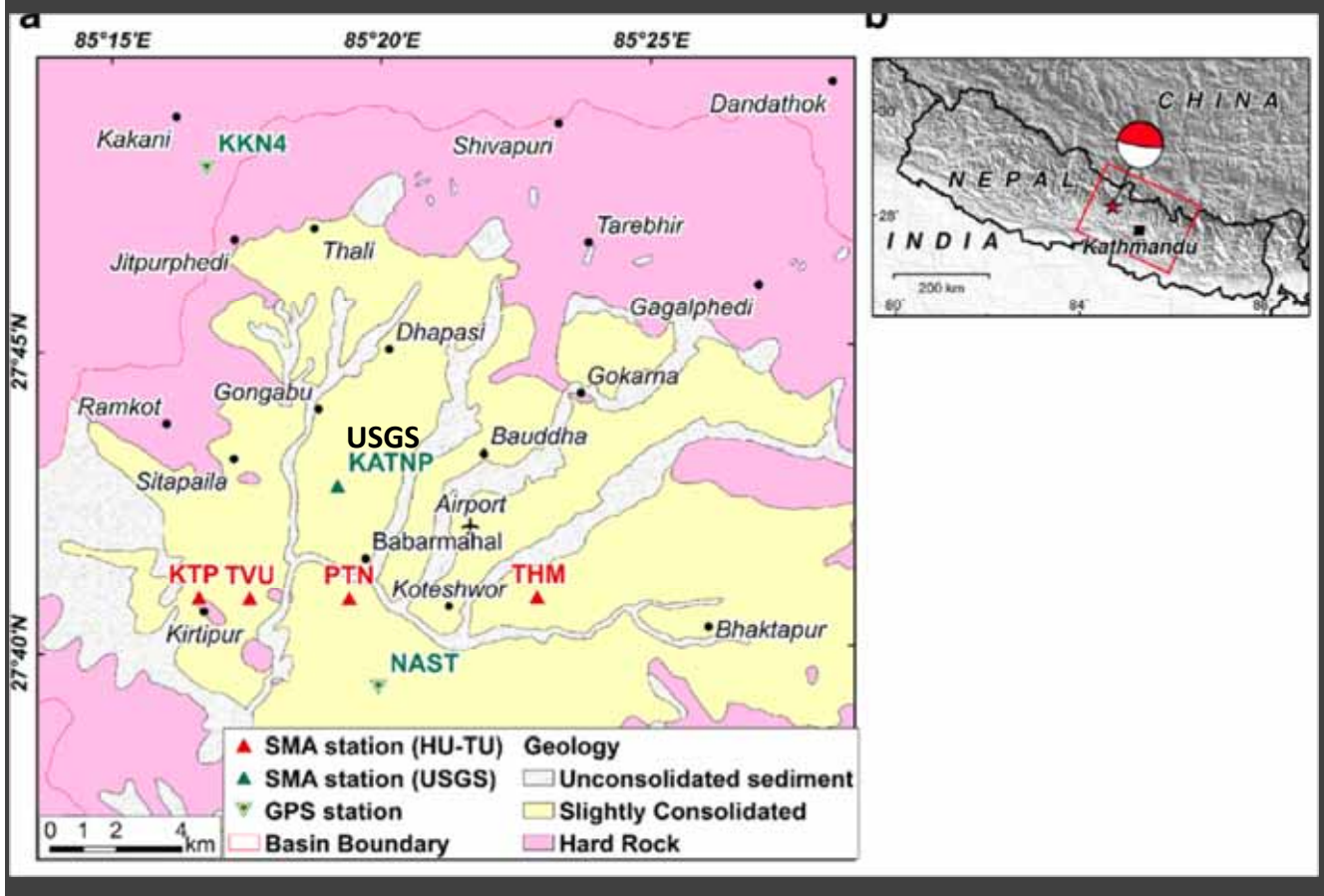
Fig. 2 Observed ground accelerations at various sites. The station at KATNP is a rock site and the others are soft sedimentary sites. The waveform shows the acceleration in cm/s² over time (0 to 120 seconds).

PGA is low—about 0.12g to 0.24g

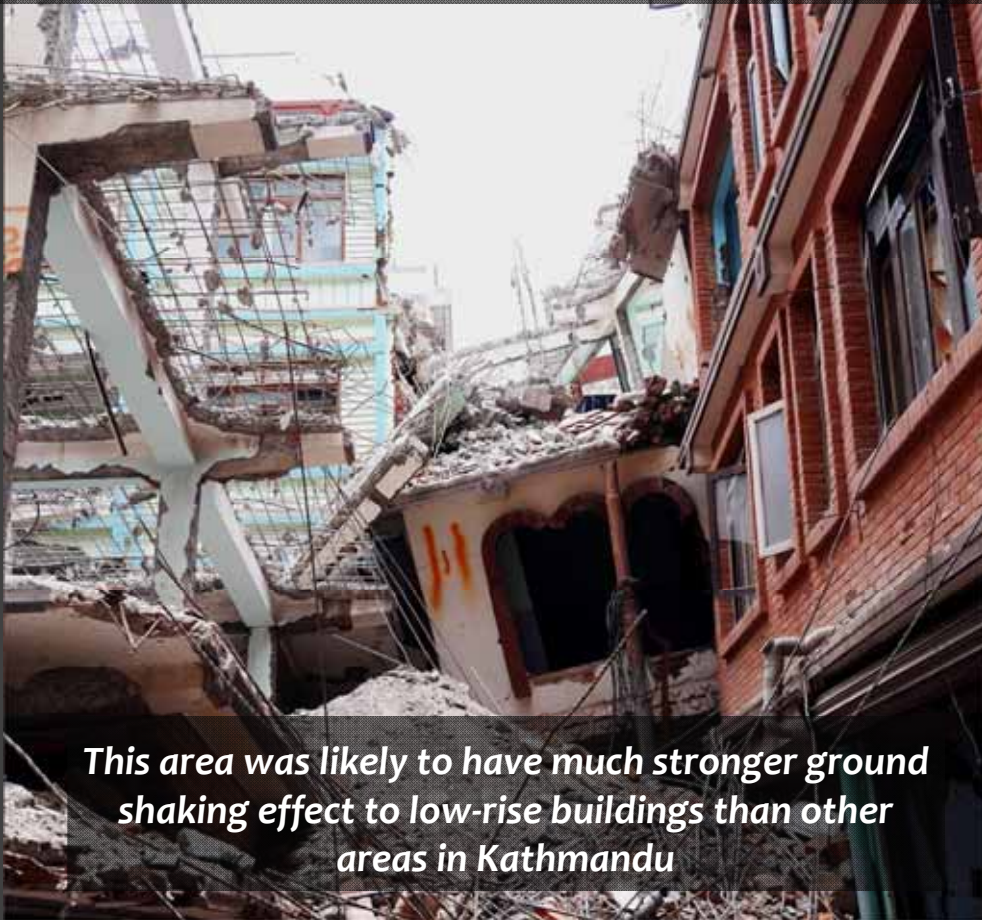
Acceleration Response Spectrum (5% Damped)



Strong-motion Accelerometer Stations in Kathmandu Valley



The Concentrated Damage Area in Gongabu, Kathmandu



This area was likely to have much stronger ground shaking effect to low-rise buildings than other areas in Kathmandu

Collapsed RC Building in Gongabu, Kathmandu



Pancake Collapse in Gongabu, Kathmandu



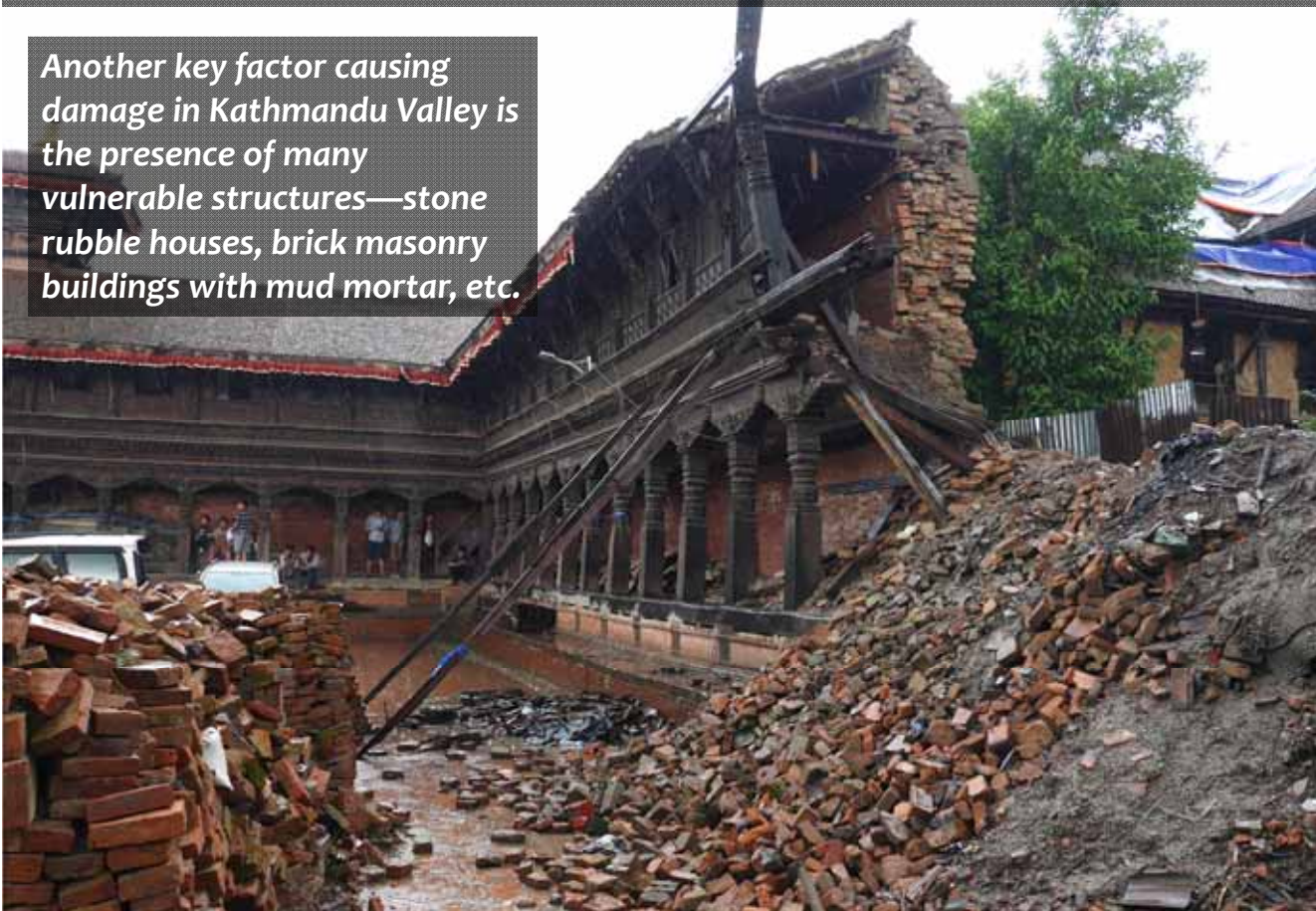
'Seismic Microzonation Study' should be properly carried out.

Low-rise buildings on 'rock sites' should be made more seismic resistant !

High-rise buildings & Long-period structures on 'basin sites' should be designed for long-period ground motions!

Bhaktapur—An Ancient City in Kathmandu Valley

Another key factor causing damage in Kathmandu Valley is the presence of many vulnerable structures—stone rubble houses, brick masonry buildings with mud mortar, etc.



Damage to Cultural Heritage Buildings in Bhaktapur

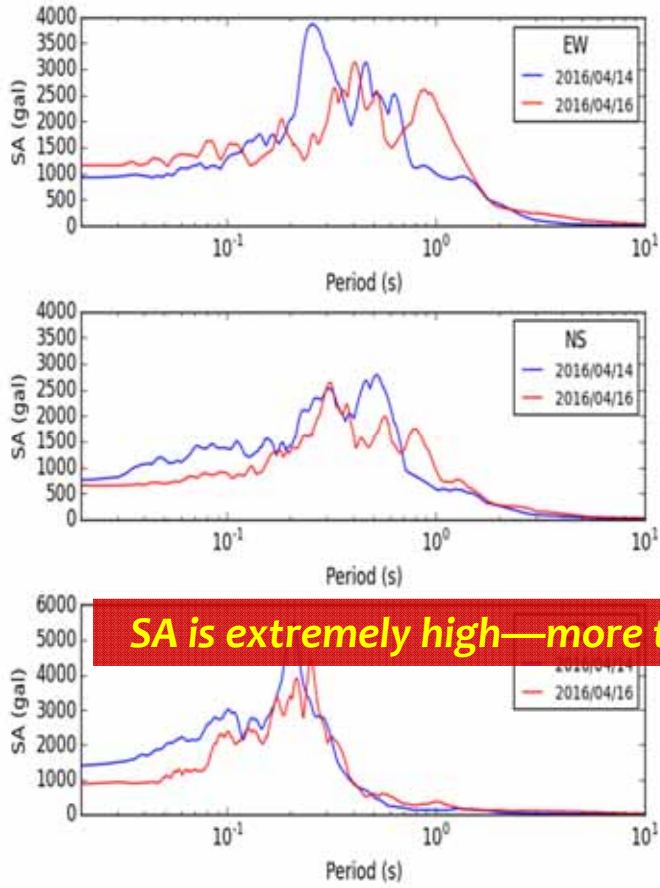


The Kumamoto Earthquakes: M 6.5 + M7.3, 14 & 16 April 2016

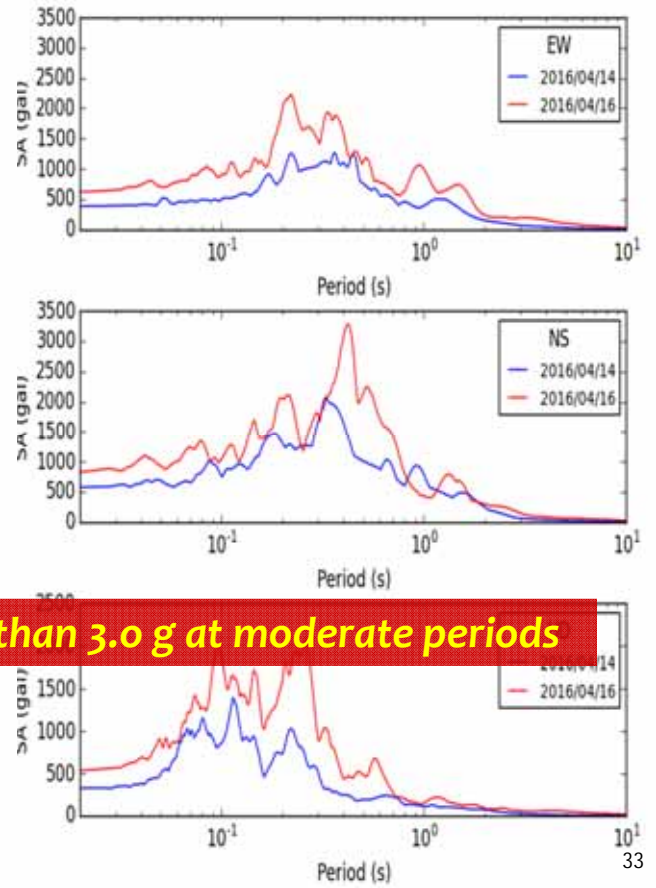


Comparison of Acc. Response Spectra for M6.5 & M7.3 EQs

KiK-net Mashiki



K-NET Kumamoto



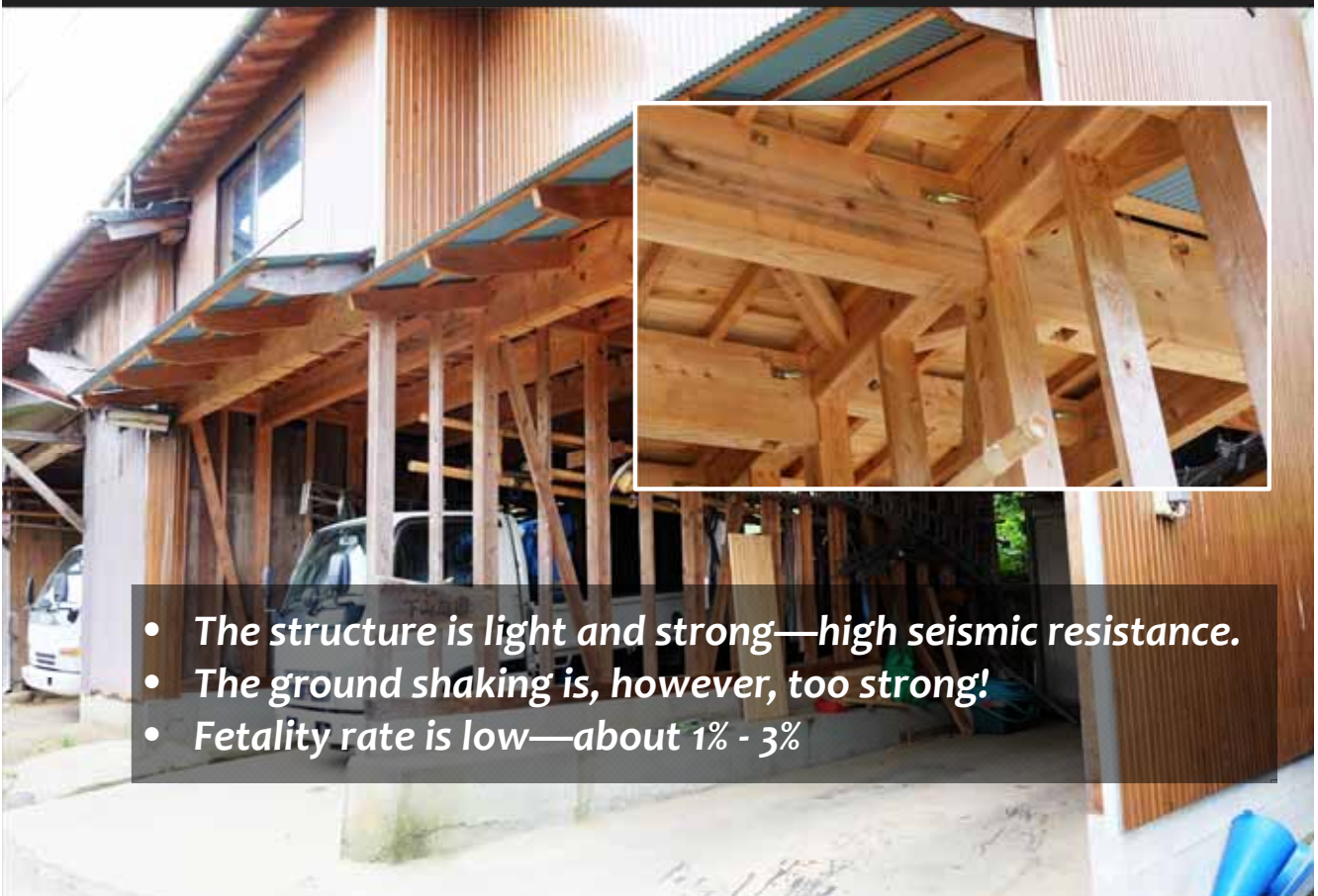
Collapse of Wooden Houses in Mashiki Town



Collapse of Wooden Houses in Mashiki Town



Typical Timber Frame & Wooden Panel of Modern Wooden Houses



- *The structure is light and strong—high seismic resistance.*
- *The ground shaking is, however, too strong!*
- *Fetality rate is low—about 1% - 3%*

Minor Damage to Some Wooden Houses in Extremely Severe Shaking Areas

